Published online 2 July 2010 *Nucleic Acids Research, 2010, Vol. 38, No. 20* ***6943–6955***
doi:10.1093/nar/gkq582

Methyl CpG binding protein 2 (MeCP2) enhances photodimer formation at methyl-CpG sites but suppresses dimer deamination

Vincent J. Cannistraro and John-Stephen A. Taylor*

Department of Chemistry, Washington University, St Louis, MO 63130, USA

Received March 27, 2010; Revised June 3, 2010; Accepted June 9, 2010

ABSTRACT

Spontaneous deamination of cytosine to uracil in DNA is a ubiquitous source of C→T mutations, but occurs with a half life of ~50 000 years. In contrast, cytosine within sunlight induced cyclobutane dipyrimidine dimers (CPD's), deaminate within hours to days. Methylation of C increases the frequency of CPD formation at PyCG sites which correlate with C→T mutation hotspots in skin cancers. MeCP2 binds to ^{m}CG sites and acts as a transcriptional regulator and chromatin modifier affecting thousands of genes, but its effect on CPD formation and deamination is unknown. We report that the methyl CpG binding domain of MeCP2 (MBD) greatly enhances C=^{m}C CPD formation at a TC^{m}CG site in duplex DNA and binds with equal or better affinity to the CPD-containing duplex compared with the undamaged duplex. In comparison, MBD does not enhance T=^{m}C CPD formation at a TT^{m}CG site, but instead increases CPD formation at the adjacent TT site. MBD was also found to completely suppress deamination of the T=^{m}CG CPD, suggesting that MeCP2 may have the capability to both suppress UV mutagenesis at Py^{m}CpG sites as well as enhance it.

INTRODUCTION

Methylation of cytosine occurs specifically at CG sites in humans and is catalyzed by methyltransferase enzymes (1). DNA methylation is linked to cell differentiation and this process is mediated, in part, by the interactions of a family of transcription factors designed to recognize ^{m}CG sequences (2). These proteins are known, collectively, as methyl-CpG binding proteins and interact with additional gene regulators (3). MeCP2 is a member of this family of proteins and promotes 'gene silencing' through its interaction with Sin3 and histone deacetylase (4,5). Although initially thought to be involved only in gene repression, it has been proposed that MeCP2 also acts a transcriptional 'up' regulator affecting the expression of thousands of genes (6). MeCP2 also plays some role in chromatin repression with the SWI/SNF chromatin-remodeling complex (7), DNA looping (8) and has been shown to cause compacting of chromatin *in vitro* (9–11). The loss in MeCP2-DNA recognition has also been linked to Rett syndrome, a form of autism and has been the focus of intense study in recent years (12).

MeCP2 is found in almost all tissues including skin (13,14) and methylation of C has also been linked to sunlight induced C → T transition mutation hotspots at dipyrimidine sites in the p53 gene of skin cancers (15–19). Methylation of cytosine greatly enhances *cis*-syn cyclobutane pyrimidine dimer (CPD) formation at dipyrimidine sites (20,21), though the resulting CPD is only weakly mutagenic toward Y family DNA polymerases (22–24). Dimer formation, however, greatly enhances the deamination of the ^{m}C to T within the dimer, which is highly mutagenic (Figure 1). Whereas deamination of ^{m}C to T occurs with a $t_{1/2}$ of ~38 000 years (25), deamination of C or ^{m}C in a CPD occurs within hours to days (26–28). Transdimer DNA synthesis by the Pol Y family polymerase pol η is known to insert A opposite the deaminated ^{m}C which would explain the origin of the observed C → T mutations (24,29,30).

DNA binding proteins are well known to modulate DNA photoproduct formation, which forms the basis of the photofootprinting technique for detecting protein DNA interactions *in vivo* (31,32). Studies with nucleosome core particles have shown that the frequency of CPD formation is modulated by its phase with respect to the nucleosome and has been attributed DNA curvature (33,34). Transcription factors have also been found to modulate CPD photoproduct formation *in vivo* and *in vitro* (35–37). The consensus model is that protein interactions change the relative positions of neighboring pyrimidines in a way to either promote or inhibit the formation of photoproducts (38,39). The effect of methyl-C binding proteins, such

*To whom correspondence should be addressed. Tel: +1 314 935 6721; Fax: +1 314 935 4481; Email: taylor@wustl.edu

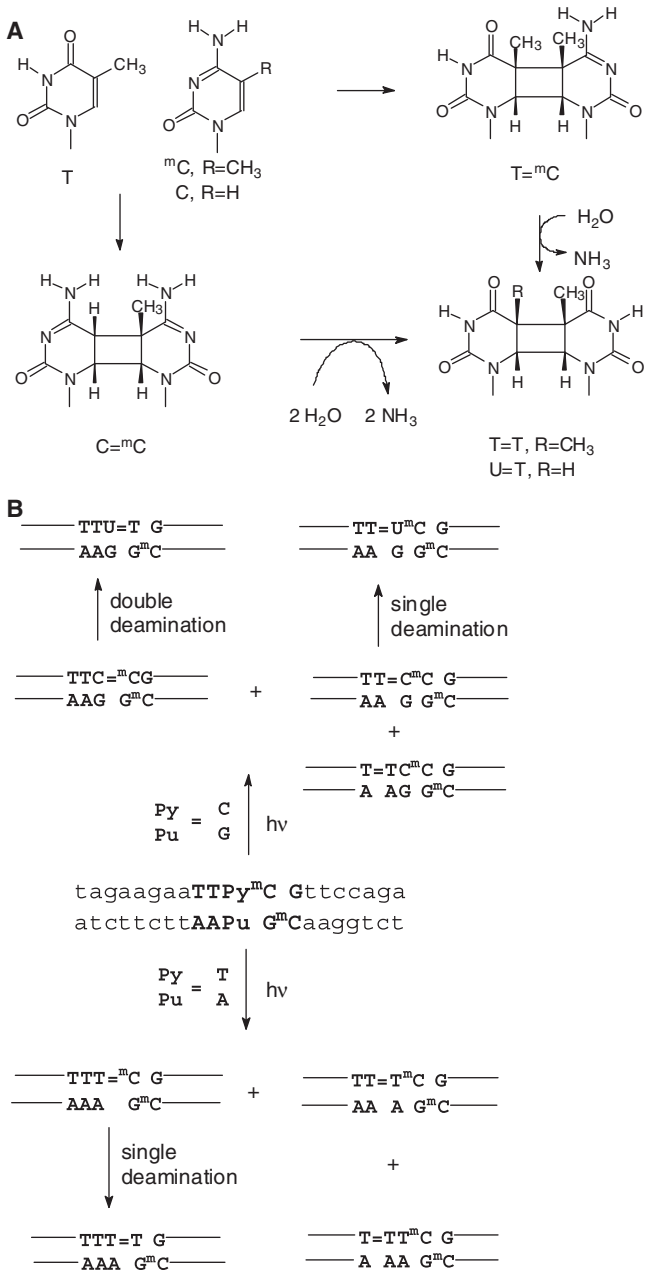

Figure 1. Cyclobutane pyrimidine dimers of Py^{m}CG sites and their deamination products. (**A**) Absorption of the UVB in sunlight by 5-methylcytosine causes *cis*-syn cyclobutane pyrimidine dimer (CPD) formation at Py^{m}CG sites (signified by "=") which is followed by deamination within hours to days to yield U and T containing CPDs, which result in C/^{m}C → T mutations when bypassed by pol η. (**B**) Irradiation of the *BDNF* sequence (where Py•Pu is C•G) or the related sequence (where Py•Pu is T•A) produces a number of CPDs within and immediately flanking the ^{m}CG•^{m}CG binding site for the MBD of MeCP2. Deamination of C or ^{m}C within a CPD results in a U or T mismatch. This study focuses on the effect MBD on photoproduct formation and deamination, and the effect of CPD formation and deamination on MBD binding.

as MeCP2, on DNA photodimer formation or deamination is unknown.

To determine whether or not MeCP2 that is present in skin cells (13,14) could affect the formation and deamination of CPDs of Py^{m}CG we have investigated the photobiology of the well characterized complex between the human MeCP2 methyl-CpG binding domain (MBD) and the *BDNF* promoter sequence (40). CPD formation was assayed by CPD-specific cleavage with T4 endonuclease V, and the binding affinity for specific photoproducts was determined by an electromobility shift assay combined with a T4 endonuclease V assay for dimers in the shifted band. The rate of CPD deamination was measured using a newly developed photolyase/nuclease P1 coupled method for quantifying the conversion of ^{32}p^{m}dC to ^{32}pT in CPDs (28). MBD was found to cause a 5-fold increase in CPD formation at a C^{m}CG site, and to bind to the resulting CPD-containing DNA duplex with equal or higher affinity than the undamaged duplex. Complete deamination of the C=^{m}C CPD to U=T, however, strongly interfered with MBD binding. While MBD was not found to have any significant effect on CPD formation at a T^{m}CG site, it was found to greatly suppress its deamination, and bind with high affinity to the duplex containing the deaminated CPD.

MATERIALS AND METHODS

Cell lines, materials

The pET30bMecp2-76-167 for expressing WT MBD was from Dr Adrian Bird. The T4 endonuclease V was from Dr R. Stephen Lloyd and *Escherichia coli* photolyase was from Dr Aziz Sancar. T4 polynucleotide kinase was from NEB. BL21 and BL21(DE)pLysS competent cells were from Novagen. Laboratory chemicals were from SIGMA. ODNs were obtained from IDT and purified by acrylamide gel electrophoresis.

Preparation of the MeCP2, methylCpG binding domain

A PET vector (pET30bMecp2-76-167) coding for a start codon followed by amino acid codons for amino acids 76–167 and then terminating with six histidine codons was a generous gift from Dr Adrian Bird's laboratory. The plasmid was used to transform BL21(DE)pLysS cells, and protein synthesis was induced with IPTG at 30°C. After 5 h of induction, the cells were centrifuged, sonicated and purified by Ni–agarose affinity chromatography. MALDI TOF: Found: 11 103, expected 11.1 kDa. Mutants were constructed by the QuikChange site-directed mutagenesis method (Stratagene).

Electrophoretic mobility shift assays

Binding experiments were performed at 4°C in either 50 mM cacodylate or 10 mM Tris–HCl, 50 mM NaCl, 5 mM EDTA and 10% glycerin, pH 8.3. MBD was allowed to pre-incubate with the duplex DNA for 15 min prior to loading a 20 × 20 × 0.1 cm 10% 1 : 30 cross-linked native polyacrylamide gel in 45 mM pH 8.3 TBE that was run at 300 V run at 4°C. The K_d was determined by non-linear least squares fitting the fraction bound (f) versus MBD concentration to $f=f_{max} \times [MBD]/(K_d+[MBD])$ with the KaleidaGraph program.

DMS mapping

Dimethyl sulfate (DMS) (0.5 µl) was added to 50 µl of 5′-^{32}P-end labeled DNA duplex (1 µM) in 50 mM cacodylate, 50 mM NaCl, 5 mM EDTA in the presence or absence of 1.2 µM MBD at 4°C. Aliquots (10 µl) were removed at various times and quenched by the addition of 50 µl of 1.5 M sodium acetate, 1 M mercaptoethanol and 50 µg of denatured salmon sperm DNA. After the addition of 200 µl water, the DNA was precipitated by the addition of three volumes of ethanol, and ethanol precipitated a second time from 300 µl of 0.3 M sodium acetate The vacuum dried pellet was then treated with 100 µl of 1 M aqueous piperidine and heated at 90°C for 30 min after which it was evaporated to dryness at 60°C under vacuum. The dried pellet was resuspended in 80 µl of formamide dye, heated to 100°C for 5 min after which 5 µl was electrophoresed on a 20% 1 : 30 denaturing cross-linked polyacrylamide gel with 45 mM pH 8.3 TBE and 8 M urea.

Photoproduct formation

ODNs (1 µM) in 50 mM NaCl, 50 mM cacodylate, 5 mM EDTA and 20 mM DTT, pH 8.3 were irradiated in 200 µl aliquots in 1.5 ml polyethylene microcentrifuge tubes covered with an ice water pack at 302 nm from a transilluminator for 45 min with or without 1.2 µM of wild-type MBD or the Y123F mutant. For experiments in which the irradiated product was to be used for electromobility shift experiments, the sample was phenol extracted twice, ethanol precipitated and vacuum dried before resuspension in 10 mM Tris–HCl pH 8.3 and 50 mM NaCl. The sample was quick frozen on dry ice before storage at −70°C.

T4 endonuclease V digestion

After UV irradiation with or without MBD, the samples were phenol extracted twice and then ethanol precipitated by the addition of 0.3 M sodium acetate and three volumes of ethanol. After a 95% ethanol wash, the samples were vacuum dried and the re-suspended in either 50 mM sodium cacodylate or 10 mM Tris–HCl pH 8.3, 50 mM NaCl and 5 mM EDTA for a final concentration of 1 µM DNA. A 10 µl sample was treated with 0.2 µg of T4 endonuclease V for 1 h at 37°C. After the reaction, the sample was diluted in 100 µl of piperidine (final concentration, 1 M). The samples were then incubated at 90°C for 30 m, followed by evaporation under vacuum at 60°C to dryness. The dry pellet was resuspended in 60 µl formamide containing xylene–cyanol dye and 5 µg of single strand that was the same as the original ODN strand labeled in the experiment. At this point, the sample was heated to 100°C for 7 min before loading a 20% 1:30 cross-linked denaturing polyacrylamide gel in 7 M urea and 45 mM TBE gel, pH 8.3.

MBD binding affinity assay for CPD-containing DNA

Irradiated duplexes (10 nM) in 10 mM Tris–HCl, 50 mM NaCl, 5 mM EDTA and 10% glycerin were incubated for 15 min at 4°C in 100 µl aliquots with varying concentrations of MBD prior to the electromobility shift assay (EMSA) described above. After phosphorimaging, the band containing the bound complex was excised and crushed with a glass rod in a 50 ml plastic tube with 5 ml of 10 mM Tris–HCl, pH 7.5 with agitation with a stir bar overnight. The next day, the sample was centrifuged to remove acrylamide and concentrated to 300 µl at 60°C after which the solution was made up to 50 mM NaCl and a 20-fold excess of an ODN complementary to the deamination product of interest was added and phenol extracted twice to remove residual MBD and then ethanol precipitated, washed and vacuum dried. Each sample was resuspended in 100 µl 10 mM Mes buffer pH 6 and then heated overnight at 67°C to completely deaminate the C=^{m}C dimer. After deamination, each sample was brought to pH 7.5 with the addition of Tris–HCl buffer and 50 mM NaCl and 5 mM EDTA, then annealed by heating to 70°C and cooling slowly. Aliquots (20 µl) were removed for the T4 endonuclease V reaction before loading on a 20% 1:30 cross-linked denaturing polyacrylamide gel containing 45 mM pH 8.3 TBE and 7 M urea.

Deamination rate determination

The general procedure has been described in detail previously (28). Briefly, a DNA duplex was constructed containing an internal ^{32}P-labeled 5-methylcytosine by first end labeling the sequence d(^{m}CGTTCCAGA) with T4 polynucleotide kinase and then ligating to d(TAGAAG AATT) in the presence of a 10-nt scaffold complementary to both sequences. After ligation, the single-strand was purified by polyacrylamide gel electrophoresis and then hybridized to its complementary sequence. Irradiation of the duplex DNA was carried out as described above but with 5 µM DNA in the absence of MBD. After irradiation, the sample was diluted 5-fold with 50 mM NaCl, 10 mM Tris–HCl pH 7.4 and 5 mM EDTA. The final pH was brought to pH 7.1 by the addition of Mes buffer. Deamination was followed at 23°C either with or without 1.2 µM MBD. Ten microliter aliquots were removed over a 48 h time frame photoreverted with 1 µg photolyase at 1.3 cm from a 15 W blacklight for 1 h at 23°C. The sample was then digested with 7 µg nuclease P1 at 23°C for 1 h and run on a 10% 1:30 cross-linked denaturing polyacrylamide in 45 mM pH 8.3 TBE and 7 M urea to separate the ^{32}pT and ^{32}p^{m}C mononucleotides. The gel surrounding the bands corresponding to the 5′-labeled mononucleotides was removed and a 28% 1:30 crosslinked denaturing polyacrylamide gel in 25 mM citric acid and 7 M urea was poured around the remaining gel slice. Electrophoresis with this gel separates ^{32}p ^{m}C (slowest) from ^{32}pT (fastest).

RESULTS

Experimental design

Experiments were designed to answer four basic questions regarding MeCP2 photobiology. Does MeCP2 inhibit or enhance photoproduct formation at Py^{m}CG sites? Do photoproducts at Py^{m}CG sites interfere with MeCP2

binding? Does MeCP2 binding affect deamination of Py^{m}CG photoproducts? Does deamination at Py^{m}CG sites affect MeCP2 binding? To answer these questions, the effect of the methyl-CpG binding domain of MeCP2 (MBD) on the photochemistry of the *BDNF* promoter III sequence d(TAGAAGAATTC^{m}CGTTCCAGA) •d(TCT GGAA^{m}CGGAATTCTTCTA) (referred to as C^{m}CG•^{m}CGG or the C^{m}CG duplex) was investigated. This system was chosen because a high-resolution crystal structure shows that methyl-CpG binding domain binds to this sequence in a single orientation, despite the pallindromic nature of the ^{m}CG•^{m}CG site (40). DNase I footprinting experiments confirm that this same orientation is preferred in solution (41). In some experiments, the mutated sequence T^{m}CG•^{m}CGA (referred to as T^{m}CG) was used in which the C of C^{m}CG was replaced with T.

Binding affinity and specificity of MBD for ^{m}C

The methyl-CpG binding domain of MeCP2 consists of amino acids 76–167 that are identical in human and mouse and was expressed and purified as a His-tagged protein (40). Based on titration of 1 μM C^{m}CG duplex with increasing amounts of purified MBD at 4°C the amount of active MBD protein in the stock solution was estimated to be ~1 mg/ml or 100 μM (Supplementary Figure S1). The binding affinity was determined by analysis of a saturation binding curve using 5 nM C^{m}CG•^{m}CGG duplex at 4°C to give a K_d of 12.5 ± 3.5 nM, which is very similar to that of 14.7 ± 1 reported for an ^{m}CG•^{m}CG sequence in a GCAGC^{m}CGGCG sequence context (42) (Supplementary Figure S2). To confirm the specificity for ^{m}CG•^{m}CG, we titrated a d(A,T) tract containing either CG•CG or CCG•CGG (Supplementary Figure S3, left) with MBD and found that both were bound with much lower affinity (K_d's > 400 nM). In contrast, the binding affinity of MBD to the methylated version of the same duplexes ^{m}CG•^{m}CG or C^{m}CG•^{m}CGG (Supplementary Figure S3, right) had K_d's of ~15 nM confirming the strong preference for ^{m}C. DNA substrates containing ^{m}Cs show a distinct MBD–DNA band that migrates slower than the free duplex that is not seen with the C-containing DNA substrates, which dissociate during electrophoresis. DNA duplexes containing multiple non-methylated CG sequences, however, bound with intermediate affinity, with K_d's ranging between 50 and 100 nM (data not shown).

DMS footprinting reveals distinct asymmetry in MBD binding

Methylation of the N7 of guanine residues of DNA by DMS can be physically blocked by proteins and can be used to map sites of protein interaction (43). To establish a chemical signature for the orientation observed in the crystal structure and confirmed in solution by DNaseI footprinting (41), footprinting experiments with DMS were carried out on a 1:1 complex between the C^{m}CG•^{m}CGG duplex and MBD. The 1:1 complex was formed by adding 1.2 μM of active MBD with 1 μM DNA duplex (Supplementary Figure S1). At higher concentrations of MBD, more than one MBD binds to the DNA (Supplementary Figure S1, lanes 9 and 10). To determine an optimal reaction time, the methylation reaction was carried out as a function of time in the presence and absence of MBD (Supplementary Figure S4) and quantified by phosphorimage analysis. Optimal band intensity was achieved at ~60 min and this time point was used for subsequent comparative studies with wild-type and mutant MBD proteins that were acquired under identical experimental conditions. Cleavage at all three G's within the C^{m}CG•^{m}CGG binding site were significantly affected by MBD binding, as well as at G5 (Figure 2A). G10, G34 and G5 were 3.2, 2.4 and 2.2-fold enhanced, respectively, whereas G9 was ~2.4-fold inhibited (Figure 2B). The same enhancements and inhibition were obtained from linear regression analysis of the time dependent data (Supplementary Figure S5), though enhancement at G10 and G5 was more pronounced (5-fold), as was inhibition at G9 (10-fold) (Supplementary Table S1 and Figure S6) which may be the result of some unrecognized difference in experimental conditions. None-the-less the reproducible inhibition of G9 methylation is consistent with the crystal structure orientation in which there is a strong H-bonding interaction between the N7 of G9 and arginine 111 (2.65 Å N–N). The enhancement at G34 is harder to explain, since the N7 of G34 is also involved in H-bonding with an arginine (Arg133), though it appears to be weaker than between N7 of G9 and Arg111 (3.17 versus 2.65 Å N–N distance). G34 also appears to be significantly less sterically hindered than G9, and it may be that the protein can facilitate the reaction of dimethylsulfate with G34 through a hydrophobic interaction. Interactions of DMS with the protein might also explain the enhanced reactivities of both G5 and G10. Methylation of the other G's (G24, G27, G4 and G40) were not significantly affected by MBD binding (<30% change) and are located outside the binding site and/or pointing more away from the protein. DMS footprinting of the T^{m}CG•^{m}CGA sequence, in which G10 is replaced by T, gave very similar results suggesting the same orientation preference in solution.

MBD binding enhances C=^{m}CG CPD formation

T4 endonuclease V was used to quantify CPD formation in the presence and absence of MBD. This enzyme cleaves CPDs through a two step mechanism involving cleavage of the glycosyl bond of the 5′-nt of the dimer followed by β-elimination of the 3′-phosphodiester through a 3′-AP lyase activity (44). Thus 5′-NpT=pTpN-3′ would be cleaved to 5′-NpS + Thy=pTpN-3′, where S represents a sugar fragment. Heating in 1 M piperidine after the reaction removes the 3′-terminal sugar fragment S resulting in 5′-Np, which is the same type of product produced from Maxam Gilbert sequencing reactions, such as the reaction of G with dimethylsulfate followed by hot piperidine. In the initial experiments, UVB irradiation was found to inactivate MBD, which was initially surprising since heating at 100°C had no effect on its ability to bind DNA. Addition of 20 mM DTT suppressed the inactivation of MBD, presumably by inhibiting UV induced free

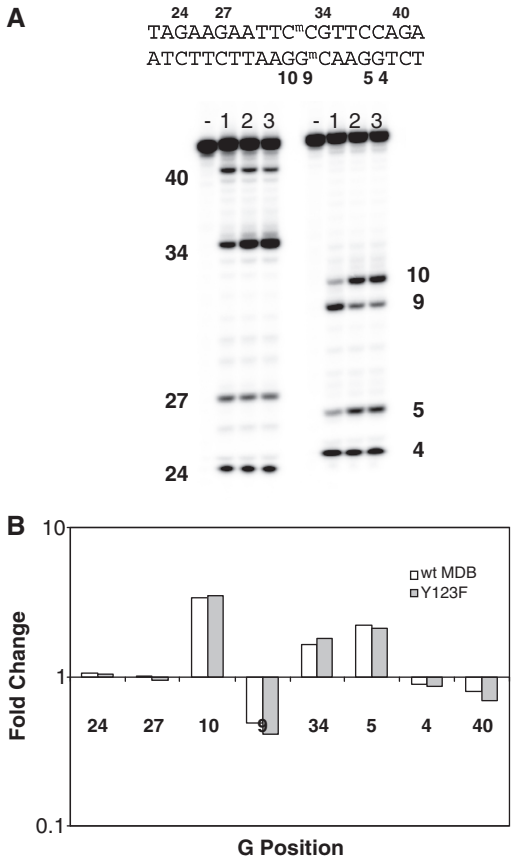

Figure 2. DMS footprinting of the MBD–DNA complex. (**A**) Denaturing gel electrophoresis of the piperidine cleavage products of a dimethylsulfate footprinting reaction carried out on the top strand (left) or the bottom strand (right) for 60 min at 4°C on the sequence shown. Lanes designated '-' are without DMS and all other lanes are with DMS. Lanes 1, 2 and 3 are with no protein, wild-type MBD and Y123F MBD, respectively. (**B**) Chart showing the log of the fold-change in G reactivity compared with the free DNA duplex. The numbers refer to the positions of the G residues in the sequence shown.

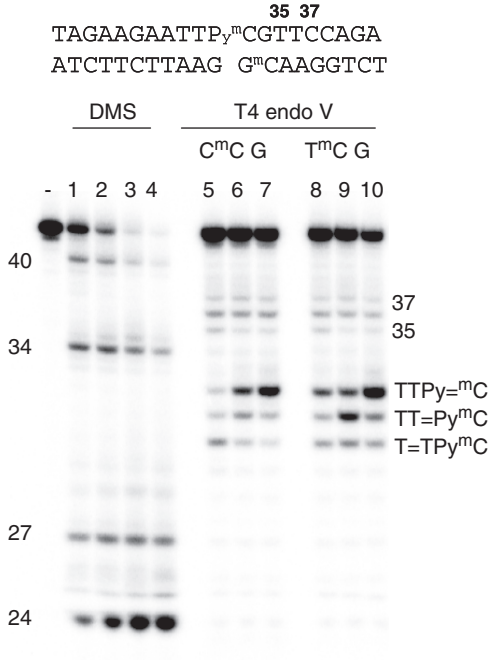

Figure 3. Modulation of UV-induced CPD formation by MBD. The DNA duplex (top) where Py was either C or T was irradiated with 302 nm UVB light in the presence or absence of MBD and then cleaved by T4 endonuclease V to reveal sites of CPDs. Lanes 5 and 8 are with no protein, lanes 6 and 9 with wild-type MBD, and lanes 7 and 10 with the Tyr123Phe mutant. The DMS reaction was also carried out on the DNA to obtain size markers (left). The lane designated '-' is without DMS. Lanes 1–4 were with DMS incubated for 10, 20, 40 and 60 min at room temperature. The numbers refer to nucleotide positions on the duplex shown in Figure 2A.

radical reactions. Addition of EDTA also suppressed inactivation of MBD to the same degree as DTT, suggesting the possible involvement of a photoredox active metal ion that may have been bound to the His-tag on the protein. In the presence of DTT, MBD was found to enhance C=^{m}C CPD formation in the C^{m}CG•^{m}CGG duplex 4.4 ± 0.3-fold (Figure 3, lane 6, Supplementary Table S2). On the other hand, MBD did not enhance T=^{m}C CPD formation in the T^{m}CG•^{m}CGA duplex, and instead enhanced formation of the neighboring T=T^{m}CG CPD 3.4 ± 1.7-fold (lane 9, Supplementary Table S2). Other proteins such as lysozyme or BSA at the same concentration did not affect photoproduct formation. MBD did not affect photoproduct formation with individual single strands, further indicating a requirement for a MBD complex with duplex DNA.

Effect of tyrosine 123 on CPD formation

Tyrosine 123 is located in the DNA binding site and interacts with the DNA by water-mediated interactions between its OH group and ^{m}C8 and the A7 phosphate in the crystal structure. Since tyrosine also absorbs UVB light and is in close proximity to the C^{m}C site, it was also possible that it might play some role in MBD photochemistry. Substituting tyrosine with phenylalanine (Y123F), which has lower UVB absorbance at 280–320 nm and is not capable of H-bonding, did not measurably affect the affinity of MBD for the C^{m}CG•^{m}CGG duplex (K_d=14 ± 3 versus 12.5 ± 3.5 nM for the WT, data not shown). The dimethylsulfate footprint also did not change significantly, except for a slight increase in the methylation of G34 (Figure 2B). Unexpectedly, phenylalanine substitution further enhanced C=^{m}CG CPD formation by 1.9 ± 0.1-fold (Figure 3, lane 7, Supplementary Table S2) for a total enhancement of 8.4-fold relative to unbound DNA. Making an additional substitution of tyrosine 120 with phenylalanine in the Y123F mutant did not change the binding affinity and had no additional effect on photoproduct yield (data not shown), most likely because Y120 is further from the DNA than Y123.

It is known that deprotonation of the phenolic OH of tyrosine (pK_a=10.2) increases its absorption maximum from 280 to 300 nm as well as abolishing its H-bond donating ability, which might have an effect on DNA photochemistry. Irradiation of the C^{m}CG•^{m}CGG duplex with MBD in pH 7.2 Tris buffer, however, resulted in the same 5-fold increase in CPD formation as was observed at pH 8.3. This result suggests that the deprotonated state of

tyrosine is not a significant contributor to the enhancement of CPD formation caused by MBD.

The effect of the Y123F mutation on the photochemistry of the T^{m}CG•^{m}CGA duplex was also investigated. As described in the previous section, wild-type MBD did not enhance T=^{m}CG CPD formation but instead increased the photoproduct yield at the adjacent TT (T=T^{m}CG) 3.4 ± 1.7-fold (Figure 3, lane 9). Rather than further enhance T=T^{m}CG CPD formation, the Y123F mutant enhanced T=^{m}CG CPD formation 2.8 ± 0.4-fold relative to the WT protein resulting in a 30% yield of CPD at this site (Figure 3, lane 10, Supplementary Table S2). This enhancement is similar to that of 1.9 ± 0.1 observed for the TC=^{m}CG indicating that this mutation only affects Py=^{m}CG dimer formation.

Assay for MBD binding to CPDs

In principle, the effect of CPD formation on MBD binding affinity could be determined by an electrophoretic mobility shift assay with a site-specific CPD-containing substrate, but at the moment there are no methods for preparing such a substrate with the length and purity required. To circumvent this problem a two-step assay was developed that couples electrophoretic mobility shift assay on irradiated DNA with T4 endonuclease V to quantify the distribution of CPDs in the shifted band. A similar type of assay has been used before to evaluate binding of a transcription factor to CPD-containing DNA (45). In the first step, the irradiated DNA is run on a native gel with increasing concentrations of MBD. In the second step the shifted band is excised, phenol extracted to remove the MBD, cleaved with T4 Endo V/piperidine and run on a denaturing gel. The relative binding affinity of MBD for a particular CPD compared to the undamaged DNA can then be determined by the relative proportion of the dimer band to the undamaged DNA band as a function of the MBD concentration. For example, if the binding affinity for the CPD was the same as that of the undamaged DNA, then the CPD-shifted band would appear in the same relative proportion as the undamaged DNA-shifted band for all MBD concentrations. Conversely, if the binding affinity of MBD for the CPD was greater than for the undamaged DNA, then the proportion of the CPD-shifted band compared with that of the undamaged DNA would be greater at lower concentrations of MBD. The proportion of CPD-shifted band would then decrease with increasing concentration until it reached the same proportion as in the original substrate. A more quantitative assessment of binding affinity can be obtained from analysis of saturation binding curve generated by multiplying the fraction of DNA shifted by MBD in the first gel by the fraction of the CPD band of interest in the shifted band for each MBD concentration.

MBD binds with equal or better binding affinity to a C=^{m}CG CPD

To determine the binding affinity of MBD for the C=^{m}CG•^{m}CGG duplex, the two gel assay described above was used. This experiment required a sufficient amount of C=^{m}CG-containing substrate, as well as precautions to prevent its deamination to single and double mismatch products (U=^{m}CG•CGG, C=TG•CGG and U=TG•CGG) during the mobility shift assay. To meet the first requirement, the C^{m}CG•^{m}CGG duplex was UVB-irradiated in the presence of Y123F MBD to produce a 19% yield of C=^{m}CG CPD, followed by phenol extraction to remove the protein. Without Y123F MBD, the CPD at this site was only produced in 2% yield, and only in 10% yield with wild-type MBD. To meet the second requirement, irradiation and subsequent manipulations were all carried out at 4°C. These precautions were deemed sufficient as the deamination half life for this C=^{m}CG CPD in a duplex was estimated to be >200 h at 37°C (28).

The mobility shift assay was then carried out with 10 nM of 5′-^{32}P-labeled UV-irradiated C^{m}CG•^{m}CGG duplex that was incubated with increasing concentrations of wild-type MBD and run on a native gel (Figure 4A). The shifted bands were extracted from the gel and phenol extracted. At this point the DNA was to be cleaved with T4 endo V/piperidine, but there was concern that under our assay conditions T4 endonuclease V might not efficiently cleave single or double-mismatched photodimer deamination products (U=^{m}CG•CGG, C=TG•CGG and U=TG•CGG) that might arise during the gel extraction process. To circumvent this potential problem, the excised products were completely deaminated by heating followed by hybridization to a 20-fold excess of an ODN that is complementary to the fully deaminated product (i.e. CAA). These products were then cleaved by T4 endo V and electrophoresed on a denaturing gel (Figure 4B). As can be seen, the ratio of the native DNA band to the T4 cleavage product band corresponding to the C=^{m}CG site was not constant over the entire range of MBD concentrations, and favored the C=^{m}CG product at low MBD concentrations. The higher ratio of the C=^{m}CG band to the C^{m}CG band at lower concentrations indicates that MBD has higher binding affinity for the C=^{m}CG photodimer than for the native DNA, which we had determined to be about 12.5 nM (see 'Binding Affinity and Specificity' section). Analysis of saturation binding curves generated by multiplying the fraction of DNA shifted by MBD in the first gel times the fraction of the product of interest in the shifted band in the T4 endonuclease gel gave K_d's of 46 ± 26 and 11 ± 3 nM for the C^{m}CG•^{m}CGG and C=^{m}CG•^{m}CGG duplexes, respectively (Figure 4C and Table 1). While there was significant error in the K_d value calculated for the undamaged DNA, it would appear that the binding affinity of MBD might be up to four times greater for photodimerized C=^{m}CG than for native C^{m}CG.

Double deamination of a C=^{m}CG CPD reduces MBD binding affinity

As discussed above, deamination of ^{m}C or C in a photodimer will produce a photodimer containing either T or U respectively that results in mismatched T•G or U•G base pairs with the complementary strand. To test whether or not mismatches resulting from deamination of

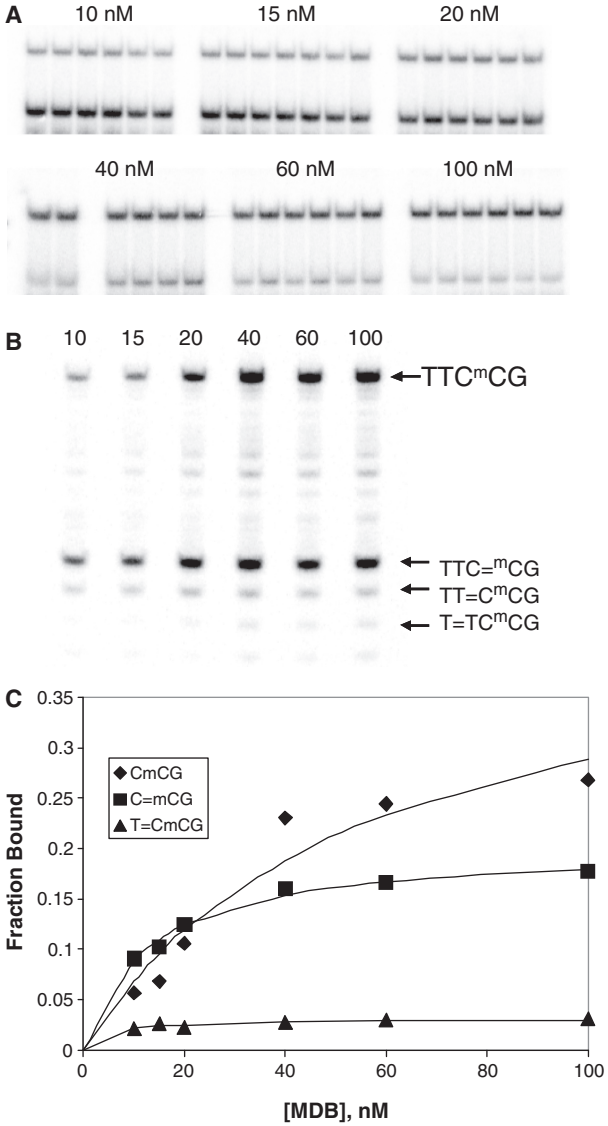

Figure 4. MBD binding affinity of CPD-containing duplexes of C^{m}CG. (**A**) Electrophoretic mobility shift assay of 10 nM UV-irradiated C^{m}CG•^{m}CGG duplex in a native gel at the indicated MBD concentrations. (**B**) Denaturing gel electrophoresis of the piperidine treated T4 endonuclease V cleavage products of the shifted bands in the gel shown in (A). The upper band is uncleaved non-dimer-containing DNA, while the lower bands correspond to cleavage of CPDs at the sites indicated. (**C**) Saturation binding curves for the undamaged DNA and dimer-containing DNA generated from the electrophoretic mobility shift and T4 cleavage data.

the C=^{m}CG CPD disrupt MBD binding, mobility shift/T4 endo V assays were carried out on mismatched CPDs. The double mismatched U=TG•^{m}CGG duplex was obtained by complete deamination of the C=^{m}CG•^{m}CGG duplex discussed in the previous section by heating. The double mismatched CPD has a much lower affinity for MBD as seen by the very small amount of the U=TG T4 endonuclease cleavage band compared to the undamaged DNA band at the highest MBD concentration of 200 nM (Figure 5B). The low binding affinity is consistent with the low binding affinity observed for the native double mismatched TTG•^{m}CGG duplex in a mobility shift assay where no shifted band was observed (Figure 5A).

Table 1. Dissociation constants for MBD•DNA complexes

TAGAAGAAnnnnGTTCCAGA
ATCTTCTTnnnn^{m}CAAGGTCT

Entry	Complex	K_d (nM)	Method
1	TTC^{m}C AAG G	12.5 ± 3.5	EMSA
2	TTC^{m}C AAG G	46 ± 26	EMSA/T4 endo
3	TTC=^{m}C AAG G	11 ± 3	EMSA/T4 endo
4	TTCT AAGG	66 ± 22	EMSA
5	TT TT AAGG	>1000	EMSA
6	TTT^{m}C AAAG	35 ± 9	EMSA
7	TTT^{m}C AAAG	75 ± 35	EMSA/T4 endo
8	TTT=T AAAG	63 ± 23	EMSA/T4 endo
9	TT=T^{m}C AA A G	13 ± 3	EMSA/T4 endo
10	T=TT^{m}C AAA G	47 ± 14	EMSA/T4

Deamination of a T=^{m}CG CPD does not affect MBD binding

The effect of a single mismatch resulting from deamination of the T=^{m}CG•^{m}CGA duplex was also investigated. A substrate containing this product was prepared by irradiation of the T^{m}CG•^{m}CGA duplex in the presence of the Y123F MBD followed phenol extraction of the protein and complete deamination with heat. The resulting product mixture was then subjected to the electromobility shift/T4 endo V assay. As can be seen from the T4 endonuclease gel and verified by phosphorimager analysis, the ratio of the cleavage bands corresponding to T^{m}CG•^{m}CGA and T=TG•^{m}CGA were relatively constant for all MBD concentrations (Figure 6A). The constant ratio indicates that MBD has the same binding affinity for the deaminated and mismatched dimer as for the non-photodamaged non-mismatched duplex, the K_d for which was independently determined to be 35 ± 9 nM. Likewise, the ratio of undamaged DNA band to the T=TT^{m}CG•^{m}CGAAA cleavage band was also relatively constant suggesting that it also had the same binding constant, presumably because the dimer is far removed from the ^{m}CG•^{m}CG binding site. More surprising, was that the cleavage band corresponding to T=T^{m}CG•^{m}CGAA was the strongest band in the 10 nM MBD T4 cleavage lane, indicating that this CPD-containing duplex bound with much higher affinity than the undamaged DNA.

A more quantitative assessment of the binding affinities could be obtained from saturation binding curves generated from the EMSA and T4 endonuclease gel data (Figure 6B). From these curves, the K_d′s for the matched TTT^{m}CG•^{m}CGAAA, mismatched TTT=TG•^{m}CGAAA,

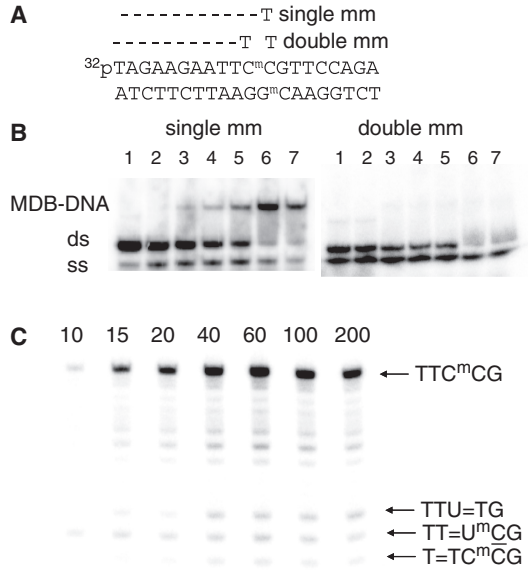

Figure 5. Binding of MBD to doubly mismatched native and CPD-containing duplexes. (**A**) Electrophoretic mobility shift assays of matched and mismatched native DNA duplexes shown with MBD. Lanes 0–8 were with 0, 10, 30, 60, 100, 200 and 300 nM MBD, respectively. (**B**) T4 endonuclease V cleavage products of MBD shifted irradiation products of the $C^mCG•^mCGG$ duplex following complete deamination.

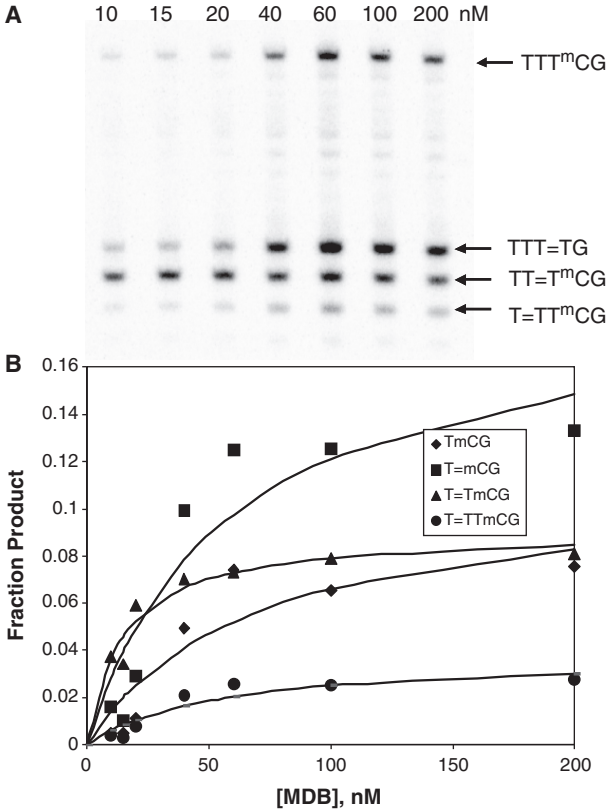

Figure 6. Binding of MBD to a singly mismatched CPD-containing duplex. (**A**) Piperidine treated T4 endonuclease V cleavage products of MBD shifted irradiation products of the $T^mCG•^mCGA$ duplex following complete deamination. (**B**) Saturation binding curves for undamaged and CPD-containing products.

and matched $TT=T^mCG•^mCGAAA$ and $T=TT^mCG•^mCGAAA$ duplexes were determined to be 75 ± 35, 63 ± 23, 13 ± 3 and 47 ± 14 nM, respectively (Table 1). The K_d of 75 ± 35 nM determined in this way for the matched $T^mCG•^mCGA$ duplex compares favorably with the K_d of 35 ± 9 nM determined directly from an electrophoretic mobility shift assay on the undamaged duplex alone. The high binding affinity for the mismatched $T=TG•^mCGA$ sequence (K_d=63 ± 23 nM) also correlates well with the binding affinity determined for the undamaged single mismatched sequence, $CTG•^mCGG$, which was found to have a K_d of 66 ± 22 nM (Figure 6A). The minimal effect of a mismatched T•G versus a matched $^mC•G$ compares well with another study which found that MBD had about the same dissociation constant for a mismatched $TTG•^mCGG$ duplex as for the matched $T^mCG•^mCGG$ duplex (17.5 ± 2.0 versus 14.7 ± 1.0 nM) (42).

MBD inhibits deamination of a T=^{m}C CPD

Having established that MBD can bind to Py=^{m}CG CPDs with high affinity, it was of interest to determine whether or not MBD binding would affect the rate of deamination. To determine the deamination rate of $T=^mCG•CGA$ CPD in the presence and absence of MBD, we made use of a recently developed two-step assay involving internal ^{32}P-labeling of the ^{m}C (28). Briefly, the method involves irradiating DNA which is 5′-^{32}P-labeled ^{m}C at the CPD site, followed by deamination for various times, enzymatic photoreversal and degradation to ^{32}pT and $^{32}pd^mC$ which are then separated and quantified. The separation of the mononucleotides requires two gel electrophoresis steps. First, a denaturing gel is used to separate the mononucleotides from protein and photoproduct-containing trinucleotides and incompletely digested products. Then a pH 3.5 citrate gel is used to separate the ^{32}pT resulting from deamination from the $^{32}pd^mC$. The relative amounts of ^{32}pT and $^{32}pd^mC$ bands are quantified by phosphorimaging, and the fraction of pT relative to that produced by complete deamination are fit to a first-order deamination rate process.

To determine the deamination rate required that MBD be stable over the time of the experiment, and devoid of contaminating enzymatic activities that could also degrade the protein or DNA. MBD was found to be stable to boiling for 10 min and further experiments showed that there was no loss of binding activity after 40 h at either 23 or 37°C. Though the preparation contained a small amount of DNase activity, it could be completely suppressed by the addition of 5 mM EDTA in the binding buffer. Even though the preparation contained some alkaline phosphatase activity, it would not affect the rate measurements because an internally labeled substrate was used. Unfortunately, the deamination half-life of $C=^mCG•^mCGG$ CPD is ~200 h at 37°C in low-salt buffer (28) and was expected to be 2-fold longer in 50 mM NaCl used in the MBD binding buffer. Based on the temperature dependence of deamination, the half life was expected to be an additional 5-fold longer if conducted at 23°C needed to help stabilize the MBD

protein its complex with the DNA. If MBD were also to inhibit deamination, as expected, the time course needed to determine the deamination rate would likely be much longer than the half-life of the MBD protein and DNA. On the other hand, deamination of T=^{m}CG•^{m}CGA was expected to be much faster, with an estimated $t_{1/2}$ of ~60 h at 23°C in 50 mM NaCl based on a known half-life of 6 h at 37°C in low-salt buffer (28). As shown in the previous section, MBD binds the mismatched CPD duplex with a K_d of 58 ± 34 nM, suggesting that the matched duplex would bind with equal or higher affinity.

The ^{32}P-labeled ^{m}C substrate was prepared by ligation of d(TAGAAGAATTT) to 5′-^{32}P-endlabeled d(^{m}CGTTC CAGA) on a shorter complementary scaffold, followed by electrophoresis to isolate the ligated product. The radiolabeled strand was annealed to its complementary strand, irradiated and then allowed to deaminate for various times with or without MBD. Following deamination, the *cis*-syn photodimers were photoreverted with *E. coli* photolyase and degraded with nuclease P1 to generate ^{32}pd^{m}C and ^{32}pT which were then separated on a citrate gel (Figure 7A and B). Neither enzymatic reaction was affected by the presence of MBD in control experiments. The deamination half-life for free T=^{m}CG CPD was determined to be 45 h (Figure 7C) and close to the estimated value of 60 h based on the presence of 50 mM NaCl and a temperature of 23°C. We were unable, however, to detect any measurable deamination for samples incubated with MBD even after exposing the gel for a much longer time (Figure 7B) indicating that MBD binding greatly suppressed deamination.

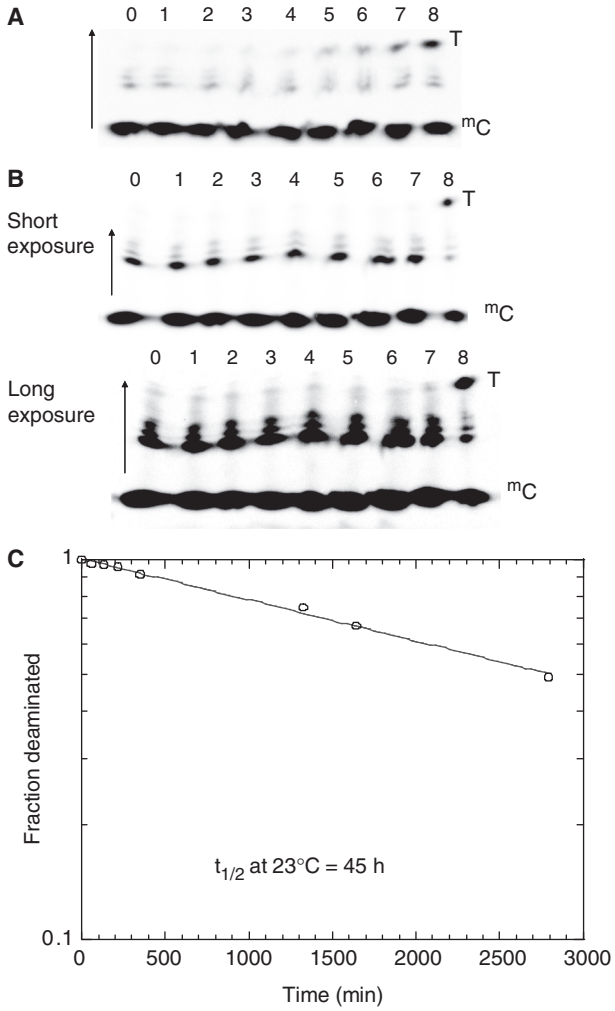

Figure 7. MBD binding suppresses ^{m}C to T deamination in a T=^{m}CG photodimer. Phosphorimage of the second dimension of a combined enzymatic two-dimensional gel electrophoresis assay of *T*=^{32}p^{m}CG•^{m}CGG dimer deamination in the presence and absence of MBD, showing the production of ^{32}pT from deamination of T=^{32}p^{m}C, photoreversal and nuclease P1 digestion (see text for explanation). Deaminations were carried out 23°C for 0, 57, 135, 221, 353, 1328, 1640 and 2793 min (lanes 1–7) in the (**A**) absence and (**B**) presence of MBD. The arrow indicates the direction of the gel and two exposures are shown for (B) showing no significant formation of pT. Lane 8 is a sample that was allowed to completely deaminate overnight at 70°C from which the fraction deaminated can be calculated. (**C**) A plot of fraction undeaminated T=^{m}C versus time calculated from the fraction deaminated. Bands appearing in between the pT and pd^{m}C bands are due to some incompletely digested oligomers, possibly containing other non-revertible photoproducts, and do not affect the rate calculation.

DISCUSSION

The efficiency for forming sunlight induced mutations at a specific site depends on a multitude of factors and competing processes. Of most importance are the types and frequencies of photoproducts produced, the frequency that photoproducts are converted to other photoproducts, the frequency that primary and secondary photoproducts are detected and repaired, and the frequency and mutagenicity of translesion synthesis by polymerases. The major class of photoproducts induced by sunlight is the *cis*-syn cyclobutane dimer of Py^{m}CG sites (46). This product is not very mutagenic on its own, but becomes highly mutagenic following deamination of a C or ^{m}C within the dimer to a U or T, which would cause C→T mutations after trans lesion synthesis by polymerase η (24).

The frequency of CPD formation has been proposed to depend on the degree to which the 5,6 double bonds of the two pyrimidines overlap (38). Recent experiments have shown that a thymine dimer is produced in <1 ps following UV excitation, which is faster than DNA can change conformation (47). This suggests that photoproduct yield is related to the proportion of photo-reactive conformations that exist at the time of light absorption. This idea is supported by molecular dynamics calculations correlating thymine dimer yield with conformation (48). Protein binding has been known for a long time to modulate photoproduct formation and is the basis of the photofootprinting technique for detecting protein DNA interactions *in vivo* (31).

Many transcription factors have been found to affect photoproduct yield (35–37,49,50), presumably by altering the conformational degrees of freedom of adjacent pyrimidines in such a way as to either inhibit or promote photoproduct formation. For example, a transcription factor might either enforce a photoreactive conformation or increase the proportion of photoreactive

conformation by destabilizing the duplex form, thereby increasing the degrees of freedom of the adjacent bases. The DNA conformation model is based on the many observations showing that transcription factors affect DNA structure. The TATA binding protein is one well characterized example. This transcription factor induces a severe bend in the DNA (51) that enhances (6,4) photoproduct formation (50,52). *In vivo* photofootprinting studies have revealed many sites of inhibition and enhanced formation of CPDs in the c-jun, c-fos and PCNA promoters, including some sites that showed upward of 25-fold enhancement of CPD formation (36). *In vitro*, TFIIA has been found suppresses dimer formation at six sites and enhance dimer formation at only one site by >40% (37).

Unlike many other transcription factors, MBD only recognizes and binds to a short dinucleotide sequence and does not cause a radical change in DNA structure (40) that could explain why C^{m}C CPD formation would be enhanced. For a photodimer to form, the C5,C6 double bonds of the two pyrimidines must overlap, but in the crystal structure, the C5–C6 double bond of the ^{m}C aligns more closely with the C1′–N1 bond than with the C5–C6 double bond of the C. Likewise the C5–C5 and C6–C6 distances of 4.5 and 4.8 Å, respectively (Figure 8A and Table 2), are outside the range considered dimerizable from molecular dynamics calculations (average upper limit of 3.6 Å) (48). It is possible, however, that this structure does not reflect either the structure or the range of accessible conformations in solution, and that MBD binding might actually increase the proportion of photoreactive conformations compared to unbound DNA. The increase in photoproduct yield upon mutating tyrosine 123 to phenylalanine might be explained by a conformational model in which removing the phenolic OH disrupts some key water-mediated interactions with the DNA that could increase its flexibility. It is also possible that the loss or alteration of these interactions could affect the absorptivity or excited state properties of C32 or ^{m}C33, though the tyrosine most closely interacts with C8 on the opposite strand.

Inspection of the other dipyrimidine sites in the crystal structure of MBD bound to the *BDNF* sequence indicates that the TC dipyrimidine site in TC^{m}C has much better overlap between the C5,C6 double bonds than in the C^{m}C site (Figure 8B versus A) and is similar to that of a T = T CPD (Figure 8D) (53). The C5–C5 and C6–C6 bond distances of 3.97 and 4.10 Å are almost within the dimerizable range (3.6 Å) (48), whereas the corresponding distances at the flanking TT site (Figure 8C) are 4.47 and 4.66 Å (Table 2). This might explain the increase in CPD yield at the TC site of TTC^{m}CG relative to the TT site upon MBD binding (Figure 3, lane 6) though this is hard to confirm without knowing the structure of the unbound DNA. The yield of CPD at the corresponding site in TTT^{m}CG (TT=T^{m}CG) increases much more dramatically, but not at the T^{m}CG site (Figure 3, lane 9).

CPDs generally inhibit binding of transcription factors to their recognition sequence. For example, CPDs were found to reduce the binding affinity of the E2F, NF-Y, AP-1, NFκB and p53 transcription factors by 11–60-fold

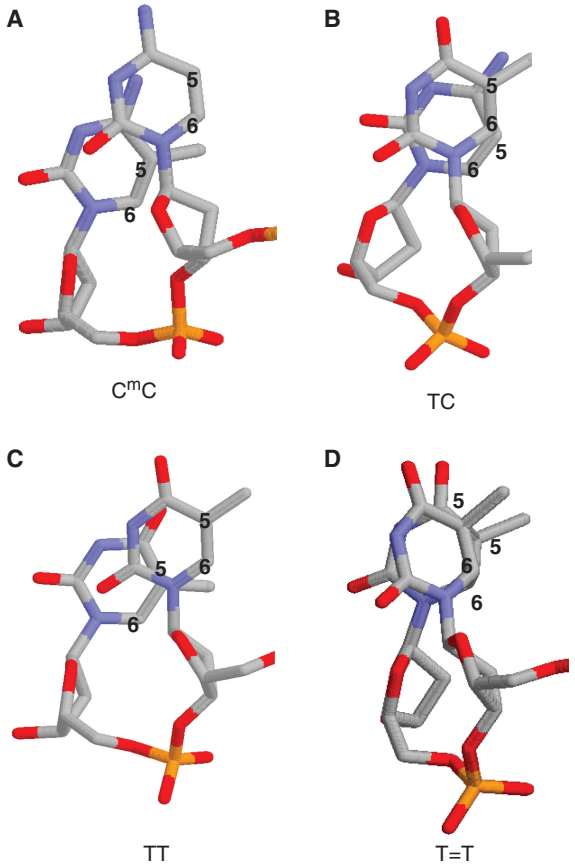

Figure 8. Base pair overlaps for dipyrimidine sites in MBD•DNA and a thymine dimer. Rasmol generated structures for the (**A**) $C^{m}_{32}C_{33}$, (**B**) $T_{31}C_{32}$ and (**C**) $T_{30}T_{31}$ steps of the TTC^{m}C sequence in the crystal structure of the *BDNF* promoter sequence complexed with MBD (3C2I.pdb), and (**D**) the thymine dimer (T=T) from the thymine dimer decamer duplex crystal structure (chain B of 1N4E.pdb).

Table 2. Distances and improper torsion angles for dipyrimidine sites in the TTC^{m}C site of the *BDNF* promoter DNA•MBD crystal structure compared with a thymine CPD in a decamer duplex crystal structure

Site	C5–C5	C6–C6	Average bond length	C5–C6–C6–C5 improper bond torsion angle
C^{m}C	4.54	4.8	4.67	30
TC	3.97	4.10	4.04	42.4
TT	4.47	4.66	4.57	38.7
T=T	23.3	1.50	1.54	23.3

(54). The effect was much less pronounced for TFIIIA, and at the one site that CPD formation was found to have been moderately enhanced, there was essentially no effect of CPD formation on binding (55). MBD appears to be unusual compared to most transcription factors since it binds to DNA containing the CPD that it promotes with equal or greater affinity than the undamaged DNA. It may be that the binding affinity of MBD for the C=^{m}CG CPD is unaffected by the dimer because MBD only recognizes the central ^{m}CG•^{m}CG dinucleotide, and that the conformation of this dinucleotide may be largely

unaffected by photodimerization. Inspection of the crystal structure of a thymine dimer reveals that while the 5′-T is unusually twisted and does not form a planar base pair, the 3′-T (53), that would correspond to the ^{m}C in the C=^{m}CG dimer, is not twisted, and forms a relatively coplanar base pair. The ability of MeCP2 to bind to a CPD within its recognition site with high affinity contrasts with the greatly destabilizing effects of oxidative damage to the G (8-oxoguanine) or to the methylC (5-hydroxymethylC) (42) on MeCP2 binding. Binding may also inhibit repair, as has been found with transcription factors (56).

Deamination of the C=^{m}C CPD to form a double mismatched base pair, however, dramatically reduces the binding affinity of MBD for the DNA as does a double mismatch in native DNA (Figure 5B and C). A single mismatch resulting from the deamination of T=^{m}CG•^{m}CGA dimer resulting in T=TG•^{m}CGA, however, does not appear to affect binding by MBD. MBD was found to have about the same affinity for the matched undeaminated and mismatched deaminated photodimer, as well as for the mismatched undimerized TTG•^{m}CGA. The ability to bind a mismatched TG•^{m}CG site as well as a matched ^{m}CG•^{m}CG site has also been observed in another sequence context, suggesting that the presence of the two G's and two methyl groups on T and/or ^{m}C is sufficient for high affinity binding (42).

It has been previously shown that α/β-type small, acid-soluble proteins (SASPS) from *Bacillus subtilis* are able to suppress cytosine deamination in native DNA by about a factor of 10, presumably by shielding the cytosine from attack by water (57). These SASP proteins are also known to suppress CPD formation, and thus function to protect spore DNA from damaging agents (58,59). Considering that MBD binds to the C=^{m}CG CPD with equal or better affinity than for the corresponding native DNA, it was expected that MBD might also inhibit deamination. Indeed, MBD was found to greatly inhibit deamination by a tandem gel assay that we recently developed for this purpose (Figure 7). Deamination of CPDs is an acid-catalyzed reaction that involves attack of water on the C4 carbon of protonated C (60). Though it would be reasonable to assume that binding of a protein would inhibit deamination by blocking access to attack by water, this outcome could not have been predicted with certainty for MBD. One of the unusual features of this protein–DNA complex is the large number of water-mediated interactions between the protein, and the C and ^{m}C (40). It may be, however, that these waters are tightly bound and not free to attack the ^{m}C, and further restrict the free movement of water within the DNA binding site (40).

The ability of MeCP2 MBD to inhibit deamination of Py=^{m}CG dimers would therefore also be expected to prevent ^{m}C→T mutations that would arise from DNA synthesis past the deaminated dimers until the CPD is repaired, presumably during replication. Thus, the MeCP2 protein might serve as UV mutation suppressor at ^{m}CG sites. The extent that it could do so, however, would depend on its ability to bind to the Py^{m}CG CPD, which could in turn be affected by chromatin structure and nucleosome positioning, and by other methylC and DNA binding proteins.

In summary, the MBD enhances CPD formation at a C^{m}CG site, binds with equal affinity to the dimerized site, and suppresses deamination of an ^{m}C within a dimer. Thus while photodimer formation may not affect MeCP2 function, MeCP2 may have opposing effects on UV hotspot formation at methyl-CpG sites. On one hand, MeCP2 might enhance UV mutations by enhancing photodimer formation and blocking access to repair enzymes, but on the other hand, it might suppress UV mutations by inhibiting the deamination step required for the photoproduct to become mutagenic. Which of these opposing effects will prevail for a particular site is likely to depend on the biological interactions and activity of the site, and remain to be elucidated.

SUPPLEMENTARY DATA

Supplementary Data are available at NAR Online.

ACKNOWLEDGEMENTS

We thank Dr Adrian Bird for the gift of the MeCP2 MBD expression vector; Stephen Lloyd for a generous gift of T4 endonuclease V; and Aziz Sancar for a generous gift of *E. coli* photolyase.

FUNDING

Funding for open access charge: National Institutes of Health (Grant CA40463).

Conflict of interest statement. None declared.

REFERENCES

1. Goll,M.G. and Bestor,T.H. (2005) Eukaryotic cytosine methyltransferases. *Annu. Rev. Biochem.*, **74**, 481–514.
2. Hendrich,B. and Bird,A. (1998) Identification and characterization of a family of mammalian methyl-CpG binding proteins. *Mol. Cell Biol.*, **18**, 6538–6547.
3. Lewis,J.D., Meehan,R.R., Henzel,W.J., Maurer-Fogy,I., Jeppesen,P., Klein,F. and Bird,A. (1992) Purification, sequence, and cellular localization of a novel chromosomal protein that binds to methylated DNA. *Cell*, **69**, 905–914.
4. Jones,P.L., Veenstra,G.J., Wade,P.A., Vermaak,D., Kass,S.U., Landsberger,N., Strouboulis,J. and Wolffe,A.P. (1998) Methylated DNA and MeCP2 recruit histone deacetylase to repress transcription. *Nat. Genet.*, **19**, 187–191.
5. Nan,X., Ng,H.H., Johnson,C.A., Laherty,C.D., Turner,B.M., Eisenman,R.N. and Bird,A. (1998) Transcriptional repression by the methyl-CpG-binding protein MeCP2 involves a histone deacetylase complex. *Nature*, **393**, 386–389.
6. Chahrour,M., Jung,S.Y., Shaw,C., Zhou,X., Wong,S.T., Qin,J. and Zoghbi,H.Y. (2008) MeCP2, a key contributor to neurological disease, activates and represses transcription. *Science*, **320**, 1224–1229.
7. Harikrishnan,K.N., Chow,M.Z., Baker,E.K., Pal,S., Bassal,S., Brasacchio,D., Wang,L., Craig,J.M., Jones,P.L., Sif,S. *et al.* (2005) Brahma links the SWI/SNF chromatin-remodeling complex with MeCP2-dependent transcriptional silencing. *Nat. Genet.*, **37**, 254–264.
8. Yasui,D.H., Peddada,S., Bieda,M.C., Vallero,R.O., Hogart,A., Nagarajan,R.P., Thatcher,K.N., Farnham,P.J. and Lasalle,J.M.

(2007) Integrated epigenomic analyses of neuronal MeCP2 reveal a role for long-range interaction with active genes. *Proc. Natl Acad. Sci. USA*, **104**, 19416–19421.
9. Georgel,P.T., Horowitz-Scherer,R.A., Adkins,N., Woodcock,C.L., Wade,P.A. and Hansen,J.C. (2003) Chromatin compaction by human MeCP2. Assembly of novel secondary chromatin structures in the absence of DNA methylation. *J. Biol. Chem.*, **278**, 32181–32188.
10. Nikitina,T., Shi,X., Ghosh,R.P., Horowitz-Scherer,R.A., Hansen,J.C. and Woodcock,C.L. (2007) Multiple modes of interaction between the methylated DNA binding protein MeCP2 and chromatin. *Mol. Cell Biol.*, **27**, 864–877.
11. Horike,S., Cai,S., Miyano,M., Cheng,J.F. and Kohwi-Shigematsu,T. (2005) Loss of silent-chromatin looping and impaired imprinting of DLX5 in Rett syndrome. *Nat. Genet.*, **37**, 31–40.
12. Amir,R.E., Van den Veyver,I.B., Wan,M., Tran,C.Q., Francke,U. and Zoghbi,H.Y. (1999) Rett syndrome is caused by mutations in X-linked MECP2, encoding methyl-CpG-binding protein 2. *Nat. Genet.*, **23**, 185–188.
13. Koturbash,I., Rugo,R.E., Hendricks,C.A., Loree,J., Thibault,B., Kutanzi,K., Pogribny,I., Yanch,J.C., Engelward,B.P. and Kovalchuk,O. (2006) Irradiation induces DNA damage and modulates epigenetic effectors in distant bystander tissue in vivo. *Oncogene*, **25**, 4267–4275.
14. Uhlen,M., Bjorling,E., Agaton,C., Szigyarto,C.A., Amini,B., Andersen,E., Andersson,A.C., Angelidou,P., Asplund,A., Asplund,C. *et al.* (2005) A human protein atlas for normal and cancer tissues based on antibody proteomics. *Mol. Cell Proteomics*, **4**, 1920–1932.
15. Brash,D.E. (1991) Infectious paradigm. *Nature*, **351**, 9.
16. Ziegler,A., Leffell,D.J., Kunala,S., Sharma,H.W., Gailani,M., Simon,J.A., Halperin,A.J., Baden,H.P., Shapiro,P.E., Bale,A.E. *et al.* (1993) Mutation hotspots due to sunlight in the p53 gene of nonmelanoma skin cancers. *Proc. Natl Acad. Sci. USA*, **90**, 4216–4220.
17. Dumaz,N., van Kranen,H.J., de Vries,A., Berg,R.J., Wester,P.W., van Kreijl,C.F., Sarasin,A., Daya-Grosjean,L. and de Gruijl,F.R. (1997) The role of UV-B light in skin carcinogenesis through the analysis of p53 mutations in squamous cell carcinomas of hairless mice. *Carcinogenesis*, **18**, 897–904.
18. Ananthaswamy,H.N., Fourtanier,A., Evans,R.L., Tison,S., Medaisko,C., Ullrich,S.E. and Kripke,M.L. (1998) p53 Mutations in hairless SKH-hr1 mouse skin tumors induced by a solar simulator. *Photochem Photobiol.*, **67**, 227–232.
19. Queille,S., Seite,S., Tison,S., Medaisko,C., Drougard,C., Fourtanier,A., Sarasin,A. and Daya-Grosjean,L. (1998) p53 mutations in cutaneous lesions induced in the hairless mouse by a solar ultraviolet light simulator. *Mol. Carcinog.*, **22**, 167–174.
20. Tommasi,S., Denissenko,M.F. and Pfeifer,G.P. (1997) Sunlight induces pyrimidine dimers preferentially at 5-methylcytosine bases. *Cancer Res.*, **57**, 4727–4730.
21. Rochette,P.J., Lacoste,S., Therrien,J.-P., Bastien,N., Brash,D.E. and Drouin,R. (2009) Influence of cytosine methylation on ultraviolet-induced cyclobutane pyrimidine dimer formation in genomic DNA. *Mutat. Res./Fund Mol. Mech. Mutagen.*, **665**, 7–13.
22. Horsfall,M.J., Borden,A. and Lawrence,C.W. (1997) Mutagenic properties of the T-C cyclobutane dimer. *J. Bacteriol.*, **179**, 2835–2839.
23. Yu,S.L., Johnson,R.E., Prakash,S. and Prakash,L. (2001) Requirement of DNA polymerase eta for error-free bypass of UV-induced CC and TC photoproducts. *Mol. Cell Biol.*, **21**, 185–188.
24. Vu,B., Cannistraro,V.J., Sun,L. and Taylor,J.S. (2006) DNA synthesis past a 5-methylC-containing cis-syn-cyclobutane pyrimidine dimer by yeast pol eta is highly nonmutagenic. *Biochemistry*, **45**, 9327–9335.
25. Shen,J.C., Rideout,W.M. 3rd and Jones,P.A. (1994) The rate of hydrolytic deamination of 5-methylcytosine in double-stranded DNA. *Nucleic Acids Res.*, **22**, 972–976.
26. Tu,Y., Dammann,R. and Pfeifer,G.P. (1998) Sequence and time-dependent deamination of cytosine bases in UVB- induced cyclobutane pyrimidine dimers in vivo. *J. Mol. Biol.*, **284**, 297–311.
27. Lee,D.-H. and Pfeifer,G.P. (2003) Deamination of 5-methylcytosines within cyclobutane pyrimidine dimers is an important component of UVB mutagenesis. *J. Biol. Chem.*, **278**, 10314–10321.
28. Cannistraro,V.J. and Taylor,J.S. (2009) Acceleration of 5-methylcytosine deamination in cyclobutane dimers by G and its implications for UV-induced C-to-T mutation hotspots. *J. Mol. Biol.*, **392**, 1145–1157.
29. Johnson,R.E., Prakash,S. and Prakash,L. (1999) Efficient bypass of a thymine-thymine dimer by yeast DNA polymerase, poleta. *Science*, **283**, 1001–1004.
30. Masutani,C., Kusumoto,R. and Hanaoka,F. (1999) The XPV (xeroderma pigmentosum variant) gene encodes human DNA Polymerase eta. *Nature*, **399**, 700.
31. Becker,M.M. and Wang,J.C. (1984) Use of light for footprinting DNA in vivo. *Nature*, **309**, 682–687.
32. Pfeifer,G.P. and Tornaletti,S. (1997) Footprinting with UV irradiation and LMPCR. *Methods*, **11**, 189–196.
33. Gale,J.M., Nissen,K.A. and Smerdon,M.J. (1987) UV-induced formation of pyrimidine dimers in nucleosome core DNA is strongly modulated with a period of 10.3 bases. *Proc. Natl Acad. Sci. USA*, **84**, 6644–6648.
34. Smerdon,M.J. (1991) DNA repair and the role of chromatin structure. *Curr. Opin. Cell Biol.*, **3**, 422–428.
35. Selleck,S.B. and Majors,J. (1987) Photofootprinting in vivo detects transcription-dependent changes in yeast TATA boxes. *Nature*, **325**, 173–177.
36. Tornaletti,S. and Pfeifer,G.P. (1995) UV light as a footprinting agent: modulation of UV-induced DNA damage by transcription factors bound at the promoters of three human genes. *J. Mol. Biol.*, **249**, 714–728.
37. Liu,X., Conconi,A. and Smerdon,M.J. (1997) Strand-specific modulation of UV photoproducts in 5S rDNA by TFIIIA binding and their effect on TFIIIA complex formation. *Biochemistry*, **36**, 13710–13717.
38. Becker,M.M. and Wang,Z. (1989) Origin of ultraviolet damage in DNA. *J. Mol. Biol.*, **210**, 429–438.
39. Pfeifer,G.P. (1997) Formation and processing of UV photoproducts: effects of DNA sequence and chromatin environment. *Photochem. Photobiol.*, **65**, 270–283.
40. Ho,K.L., McNae,I.W., Schmiedeberg,L., Klose,R.J., Bird,A.P. and Walkinshaw,M.D. (2008) MeCP2 binding to DNA depends upon hydration at methyl-CpG. *Mol. Cell*, **29**, 525–531.
41. Klose,R.J., Sarraf,S.A., Schmiedeberg,L., McDermott,S.M., Stancheva,I. and Bird,A.P. (2005) DNA binding selectivity of MeCP2 due to a requirement for A/T sequences adjacent to methyl-CpG. *Mol. Cell*, **19**, 667–678.
42. Valinluck,V., Tsai,H.H., Rogstad,D.K., Burdzy,A., Bird,A. and Sowers,L.C. (2004) Oxidative damage to methyl-CpG sequences inhibits the binding of the methyl-CpG binding domain (MBD) of methyl-CpG binding protein 2 (MeCP2). *Nucleic Acids Res.*, **32**, 4100–4108.
43. Wissmann,A. and Hillen,W. (1991) DNA contacts probed by modification protection and interference studies. *Methods Enzymol.*, **208**, 365–379.
44. Lloyd,R.S. (2005) Investigations of pyrimidine dimer glycosylases–a paradigm for DNA base excision repair enzymology. *Mutat. Res.*, **577**, 77–91.
45. Carpenter,M., Divvela,P., Pingoud,V., Bujnicki,J. and Bhagwat,A.S. (2006) Sequence-dependent enhancement of hydrolytic deamination of cytosines in DNA by the restriction enzyme PspGI. *Nucleic Acids Res.*, **34**, 3762–3770.
46. Pfeifer,G.P., You,Y.H. and Besaratinia,A. (2005) Mutations induced by ultraviolet light. *Mutat Res.*, **571**, 19–31.
47. Schreier,W.J., Schrader,T.E., Koller,F.O., Gilch,P., Crespo-Hernandez,C.E., Swaminathan,V.N., Carell,T., Zinth,W. and Kohler,B. (2007) Thymine dimerization in DNA is an ultrafast photoreaction. *Science*, **315**, 625–629.
48. Law,Y.K., Azadi,J., Crespo-Hernandez,C.E., Olmon,E. and Kohler,B. (2008) Predicting thymine dimerization yields from molecular dynamics simulations. *Biophys J.*, **94**, 3590–3600.

49. Pfeifer,G.P., Drouin,R., Riggs,A.D. and Holmquist,G.P. (1992) Binding of transcription factors creates hot spots for UV photoproducts in vivo. *Mol. Cell Biol.*, **12**, 1798–1804.
50. Aboussekhra,A. and Thoma,F. (1999) TATA-binding protein promotes the selective formation of UV-induced (6-4)-photoproducts and modulates DNA repair in the TATA box. *EMBO J.*, **18**, 433–443.
51. Chasman,D.I., Flaherty,K.M., Sharp,P.A. and Kornberg,R.D. (1993) Crystal structure of yeast TATA-binding protein and model for interaction with DNA. *Proc. Natl Acad. Sci. USA*, **90**, 8174–8178.
52. Wang,Y., Gross,M.L. and Taylor,J.S. (2001) Use of a combined enzymatic digestion/ESI mass spectrometry assay to study the effect of TATA-binding protein on photoproduct formation in a TATA box. *Biochemistry*, **40**, 11785–11793.
53. Park,H., Zhang,K., Ren,Y., Nadji,S., Sinha,N., Taylor,J.S. and Kang,C. (2002) Crystal structure of a DNA decamer containing a cis-syn thymine dimer. *Proc. Natl Acad. Sci. USA*, **99**, 15965–15970.
54. Tommasi,S., Swiderski,P.M., Tu,Y., Kaplan,B.E. and Pfeifer,G.P. (1996) Inhibition of transcription factor binding by ultraviolet-induced pyrimidine dimers. *Biochemistry*, **35**, 15693–15703.
55. Kwon,Y. and Smerdon,M.J. (2005) DNA repair in a protein-DNA complex: searching for the key to get in. *Mutat Res.*, **577**, 118–130.
56. Conconi,A., Liu,X., Koriazova,L., Ackerman,E.J. and Smerdon,M.J. (1999) Tight correlation between inhibition of DNA repair in vitro and transcription factor IIIA binding in a 5S ribosomal RNA gene. *EMBO J.*, **18**, 1387–1396.
57. Sohail,A., Hayes,C.S., Divvela,P., Setlow,P. and Bhagwat,A.S. (2002) Protection of DNA by alpha/beta-type small, acid-soluble proteins from Bacillus subtilis spores against cytosine deamination. *Biochemistry*, **41**, 11325–11330.
58. Nicholson,W.L., Setlow,B. and Setlow,P. (1991) Ultraviolet irradiation of DNA complexed with alpha/{Beta}-type small, acid-soluble proteins from spores of Bacillus or Clostidium species makes spore photoproduct but not thymine dimers. *Proc. Natl Acad. Sci. USA*, **88**, 8288–8292.
59. Douki,T., Setlow,B. and Setlow,P. (2005) Effects of the binding of alpha/beta-type small, acid-soluble spore proteins on the photochemistry of DNA in spores of Bacillus subtilis and in vitro. *Photochem. Photobiol.*, **81**, 163–169.
60. Lemaire,D.G.E. and Ruzsicska,B.P. (1993) Kinetic analysis of the deamination reactions of cyclobutane dimers of dTpdC and dCpdT. *Biochemistry*, **32**, 2525–2533.